

# The Application of Mathematical Programming in Theoretical Chemistry. I. Saddle-point-search Method Applied to a $H_3$ Molecule\*

Yukio YONEDA

Department of Synthetic Chemistry, Faculty of Engineering,  
The University of Tokyo, Hongo, Bunkyo-ku, Tokyo 113

(Received December 23, 1977)

A new method to find the activated state of a reaction *without* preparing its potential energy surface was proposed and proved useful with the example of a  $H_3$  molecule. The first and the second derivatives of the total energy, with respect to every cartesian coordinate of a  $H_3$  molecule, were calculated by means of a perturbation method employing a modified EHMO. First, the bottom of the valley in the potential energy surface leading to the saddle point is sought with the aid of the quadratic approximation on the superplane on which the maximum curvature at the representative point lies. Second, the ascending path is determined to be the reverse of the steepest descending path according to the principle of microscopic reversibility. By repeating these procedures, the activated state was found without preparing the potential energy surface. The classical activation energy thus found was 8.8 kcal/mol, which is in good agreement with the experimental values.

The theoretical determination of activated state of a given reaction generally requires knowledge of the potential energy surface (PES) of the system. Quantum chemical calculations, non-empirical<sup>1)</sup> and semi-empirical,<sup>2)</sup> have been published on the gas-phase exchange reaction  $H+H_2=H_2+H$  and its isotopic variants, which belong to the simplest class of chemical reactions. In these calculations, the activated state, or the saddle point, was pinpointed on a two-dimensional contour map, because the linear complex of a  $H_3$  molecule is, fortunately, more stable than the non-linear one. The dimerization of two carbene molecules to produce an ethylene molecule<sup>3)</sup> is a yet simpler reaction; the preparation of a complete PES of the system is, however, practically impossible because of its already large degree of freedom beyond two, *i.e.*,  $6 \times 3 - 6 = 12$ ; hence, a fairly large number of calculations are necessary to obtain the total energies at the eighteen dimensional grid points. Thus, in the practical calculation, the bond distance,  $r_{CH}$ , was kept constant throughout the reaction and only a schematic diagram could be shown instead of a contour map.

Therefore, the development of a method which requires only a feasible number of calculations to obtain the reaction path is strongly desirable. By virtue of the method of optimization adopted, the method described in this paper does not require the preparation of the complete PES, and it is, therefore, particularly suitable when we need only information on the activated state and the reaction path.

Several methods of optimization, techniques in mathematical programming, have been widely employed, especially in engineering, to determine extreme value(s) without preparing a contour map of a given function; only the first derivatives (the first and second derivatives in some techniques) of the function at the successively proceeding representative point are required to arrive at the peak of the mountain.

A doctrinal formulation of reaction paths and activated states has been proposed by Fukui.<sup>4)</sup> The pur-

pose of the present work is to develop a new practical method for climbing up from the foot (the reactant) to the saddle point (the activated state) along the bottom of the valley connecting them, and then going down to another foot (the product). The simplest example, the  $H_3$  system, will be presented to demonstrate the usefulness of this method.

The energy may be calculated by means of any method, including even the molecular force field, provided that the derivatives are calculable. In this paper, the energy was calculated quantum-chemically by means of a modified extended Hückel molecular orbital (EHMO) method.

This method can also be employed in larger systems with semi-empirical MO calculations; some results with MINDO/2 and 3 will be published later.

## Theoretical

**Saddle-point Search.** The geometry of a reacting system such as  $H_3$  is described by a representative point in a  $3N_{at}$  dimensional space, where  $N_{at}$  is the number of atoms in the system. When  $q_u$  ( $u=1$  to  $3N_{at}$ ) represents every 3-dimensional cartesian coordinate of all the atoms, and  $E_b$  is the total bond energy of the system, the saddle point is defined by

$$\frac{\partial E_b}{\partial q_1} = \frac{\partial E_b}{\partial q_2} = \dots = \frac{\partial E_b}{\partial q_{3N_{at}}} = 0, \quad (1a)$$

$$\frac{\partial^2 E_b}{\partial b_r^2} < 0 \text{ and } \frac{\partial^2 E_b}{\partial b_f^2} < 0, \quad (1b)$$

$$\frac{\partial^2 E_b}{\partial b_1^2} > 0, \frac{\partial^2 E_b}{\partial b_2^2} > 0, \dots, \quad (1c)$$

where  $\partial^2 E_b / \partial b^2$  implies the second derivative of the total bond energy with respect to the bond length of a bond,  $b$ , while Eq. 1b represents the criteria of the curvatures of the PES along the rupturing bond,  $b_r$ , and the forming one,  $b_f$ , whereas Eq. 1c represents the criteria along the bonds which are not directly related to the activated state. On the other hand, the criteria of the most stable structure of a molecule, or the minimum energy geometry, are described by Eqs. 1a and 2:

$$\frac{\partial^2 E_b}{\partial q_1^2} > 0, \frac{\partial^2 E_b}{\partial q_2^2} > 0, \dots, \frac{\partial^2 E_b}{\partial q_{3N_{at}}^2} > 0 \quad (2)$$

\* CHEMOGRAM, a Computer Program Package for Chemical Logic, Part I. A preliminary report of this work was presented at the 31st National Meeting of the Chemical Society of Japan, Sendai, October, 1974.

Thus, the criteria of the saddle point in cartesian coordinates becomes as follows where Eq. 1a holds, Eq. 1d is satisfied for a few coordinates which are directly related to the rupturing or forming bonds, and Eq. 1e holds for the remaining coordinates, a majority:

$$\frac{\partial^2 E_b}{\partial q^2} < 0 \quad (\text{for a few coordinates}), \quad (1d)$$

$$\frac{\partial^2 E_b}{\partial q^2} > 0 \quad (\text{for the majority of coordinates}). \quad (1e)$$

The mathematical definition of the bottom of the valley on the PES will be discussed below. Figure 1a shows a schematic diagram of a superplane or a PES around a valley, V. P is a representative point of the system which is not at the bottom, but fairly near it. S is a superplane *orthogonal* to V, on which the point P and a curve, PQ, which is a section of S and V and which has the maximum curvature at P, are laid. The minimum point, B, on the PQ curve is the bottom of the valley near P, as is shown in Fig. 1b. The PQ curve may have its maximum curvature even at B, because P is near B. In practical calculations, the PQ curve is determined by the second derivatives of the total bond energy at P, while the location of B is estimated by the quadratic approximation with the aid of the first and the second derivatives at P. If the B thus estimated is far from P, the same procedure may be repeated to assure that the true bottom of the valley is attained.

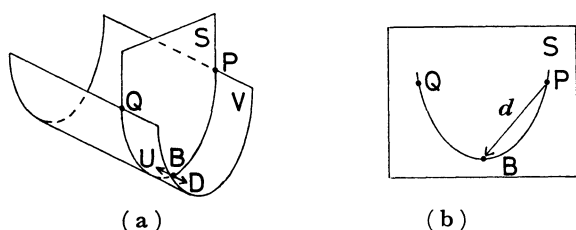


Fig. 1. Schematic diagram for saddle point search method.

- (a) Potential energy surface near a bottom of a valley.  
(b) Bottom of a valley on a superplane S.

The reaction path along the bottom of the valley, V, is determined as follows. First, the direction of the steepest descent, BD, is decided with the aid of the first derivatives at the point B. This direction leads the system to the initial geometry; hence, the path to the saddle point, BU, will be the reverse direction to BD, by the principle of microscopic reversibility. The BU distance should be small enough, say 0.05 Å, so that the above principle can be applied. Even if the BU step is short, it can not be guaranteed that the U point is still at the bottom; hence, the same procedure employed with P is applied at U before ascending further toward the saddle point.

**Modified EHMO and Its Perturbational Calculation of First and Second Derivatives.** Generally, empirical or semi-empirical MO's, such as EHMO, CNDO, INDO, or MINDO, do not give correct values of the equilibrium distance or the energy profile of a hydrogen molecule. The total electronic energy calculated by EHMO implicitly involves the nuclear repulsion ener-

gy;<sup>5)</sup> hence, the total electronic energy minus the sum of the Coulomb integrals, which are geometry-independent, gives the total bond energy. Salomon<sup>6)</sup> calculated a semi-empirical PES by means of the Heitler-London method, employing modified overlap integrals to obtain a better fit of the calculated bond energy of  $H_2$  to that of the Morse function.

By the same principle, we introduced a modified EHMO. We do not insist that this modification is a novel improvement of EHMO; we just used it as a less expensive MO, applicable only for hydrogen atoms with *s* orbitals alone, to demonstrate the validity of the present saddle-point-search method.

The resonance integrals were formulated, as is shown in Eq. 3b, to make the total bond energy as close as possible to the experimental value of a hydrogen molecule at various interatomic distances of interest:

$$\text{Coulomb integral: } H_{rr} = -13.60 \text{ eV}, \quad (3a)$$

$$\text{resonance integral: } H_{rs} = \frac{1}{2} \sum_k^w a_k |S_{rs}|^{k-1} \times S_{rs}(H_{rr} + H_{ss}), \quad (3b)$$

where *r* and *s* denote atomic orbitals. Thus, the resonance integral is expressed as a power series of an overlap integral,  $S_{rs}$ , which is calculated with the Slater orbitals by means of the Mulliken method. Then the coefficients,  $a_k$ , can be determined by the least-squares method so as to fit the Morse function.

The derivatives could be calculated by the method of finite differences from the eigenvalues of a slightly distorted system. The calculation, however, requires two extra geometries for each coordinate of an atom; thus, the number of calculations amounts to  $2 \times 3N_{at}$ , which is 18 even for the smallest system,  $H_3$ . As the computation time of the diagonalization of a secular equation usually increases nearly proportionally to  $N^{2.5-3}$ , where *N* is the number of atomic orbitals, the method of finite differences may be inappropriate for a larger system.

In the case of EHMO, the total (electronic) energy of a system is calculated from the sum of the eigenvalues of a secular equation,

$$|H^{(0)}_{rs} - \epsilon S^{(0)}_{rs}| = 0. \quad (4)$$

When a small change in one coordinate of an atom ( $\Delta q$ ) is regarded as a perturbation, the perturbed matrices, *H* and *S*, may be described by

$$H = H^{(0)} + \lambda H^{(1)} + \lambda^2 H^{(2)}, \quad (5a)$$

$$= H^{(0)} + \left( \frac{\partial H^{(0)}_{rs}}{\partial q} \right) (\Delta q) + \frac{1}{2} \left( \frac{\partial^2 H^{(0)}_{rs}}{\partial q^2} \right) (\Delta q)^2, \quad (5b)$$

$$S = S^{(0)} + \lambda S^{(1)}, \quad (5c)$$

where  $S^{(2)}$  was omitted for the sake of simplification and where parentheses denote a matrix. The total energy after perturbation, *E*, is given by

$$E = E^{(0)} + \lambda E^{(1)} + \lambda^2 E^{(2)} \quad (5d)$$

$$= E^{(0)} + (\partial E^{(0)} / \partial q) (\Delta q) + (1/2) (\partial^2 E^{(0)} / \partial q^2) (\Delta q)^2. \quad (5e)$$

Therefore, the first and the second derivatives of the total energy of the system with respect to the designated coordinate are given by

$$\frac{\partial E^{(0)}}{\partial q} = E^{(1)}, \quad (5f)$$

$$\frac{\partial^2 E^{(0)}}{\partial q^2} = 2E^{(2)}. \quad (5g)$$

Since the difference between the total bond energy,  $E_b$ , and the total energy,  $E$ , are constant, the derivatives of the former with respect to the coordinates are equal to those of the latter.

The non-zero elements of the first- and second-order perturbation matrices are given by the following equations:

First-order:

$$\frac{\partial H_{rs}}{\partial q_u} = \frac{\partial H_{rs}}{\partial S_{rs}} \cdot \frac{\partial S_{rs}}{\partial q_u} \text{ for off-diagonal,} \quad (6a)$$

$$\frac{\partial S_{rs}}{\partial q_u} \text{ for off-diagonal.} \quad (6b)$$

Second-order:

$$\frac{1}{2} \frac{\partial^2 H_{rs}}{\partial q_u^2} = \frac{1}{2} \left\{ \frac{\partial^2 H_{rs}}{\partial S_{rs}^2} \left( \frac{\partial S_{rs}}{\partial q_u} \right)^2 + \frac{\partial H_{rs}}{\partial S_{rs}} \frac{\partial^2 S_{rs}}{\partial q_u^2} \right\} \text{ for off-diagonal.} \quad (7)$$

The first and the second derivatives of overlap integral can easily be calculated with the method of finite differences by shifting the coordinate in two directions for a small distance (usually 0.05 Å). Elements of Hamiltonian perturbation matrices can be analytically calculated with ease by the use of Eqs. 3, 6, and 7. Then the perturbation energies can be calculated by the method reported by Carbo.<sup>7)</sup>

### Calculation

*Coefficients of the Modified Resonance Integral.* The parameters for the Morse function, Eq. 8, are selected as follows:

$$V = D_e [1 - \exp\{-a(r - r_e)\}]^2, \quad (8)$$

where  $D_e = -4.76 \text{ eV}$ ,  $a = 1.957 \text{ Å}^{-1}$ , and  $r = 0.7413 \text{ Å}$ .

A seven-term polynomial for Eq. 3b was chosen ( $w=7$ ), and the seven coefficients were estimated as shown below at 15 interatomic distances from  $r = 0.9r_e$  to  $2.3r_e$ :

$$a_1 = 1.0405, \quad a_2 = 0.4695, \quad a_3 = 0.6302, \quad a_4 = -1.3501,$$

$$a_5 = -0.6601, \quad a_6 = 5.8697, \quad \text{and } a_7 = -5.3563.$$

The coincidence between these two sets of values at distances of interest is satisfactory, the standard deviation of differences between them being 0.009 eV, or 0.2 kcal/mol, for this range.

*Flow Chart of Computer Program.* The computation was carried out on a HITAC 8800/8700 system at the Computer Centre of the University of Tokyo. The block-flow chart of the main program, EHMP1, is shown in Fig. 2. The input data, essentially composed of coordinates of initial system, quantum chemical parameters, constraint parameters, and control variables, are analyzed. The eigenvalues and the eigenvectors are calculated in a subroutine, EHCAL. Second, the derivatives are calculated in another subroutine, MPEHPT, following the procedure described above. Thirdly, either the bottom of the valley or the ascending path, decided by a control variable,

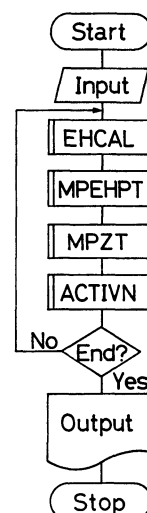


Fig. 2. Block flow chart of computer program EHMP1.

is searched with the above-mentioned algorithm stored in a third subroutine, MPZT. Finally, a fourth subroutine, ACTIVN, judges whether or not the saddle point is attained. If the system is still ascending, the procedures are repeated from EHCAL using renewed coordinates. During these iterations, the search of the bottom and that of the ascending path are repeated alternatively. If the representative point arrives at the saddle point, the coordinate is slightly changed so that the representative point is forced to move to the opposite side beyond the saddle point. Then repeated calculation from EHCAL searches the path down to the foot on the opposite side, that is, the product, by using the conventional optimization algorithm. The main program and subroutines are all written in FORTRAN IV. Some details of the procedures will now be explained.

*Algorithm in Subroutines:* The subroutine EHCAL makes use of conventional quantum chemical calculations by using the EHMO, except that the modified resonance integrals shown in Eq. 3b are used.

The details of the processing in the subroutine MPEHPT are shown in Fig. 3. The input[1] consists of the eigenvalues and eigenvectors of the unperturbed system. The following processing is iterated[2] for  $x$ -,  $y$ -, and  $z$ -coordinates down to the decision box[9]. The overlap integral matrices of unperturbed ( $S^{(0)}$ ), and the first ( $S^{(1)}$ )- and the second ( $S^{(2)}$ )-order perturbation are calculated in the subroutine MPOVLP[3]. Because the following relations hold throughout the system;

$$\partial S_{rs} / \partial q_v = -\partial S_{rs} / \partial q_w, \quad (9a)$$

$$\partial^2 S_{rs} / \partial q_v^2 = \partial^2 S_{rs} / \partial q_w^2, \quad (9b)$$

where the orbitals,  $r$  and  $s$ , belong to atoms whose coordinates along the same axis are  $q_v$  and  $q_w$  respectively, only one calculation in each iteration can give the derivatives for all atoms.

The perturbational calculation is iterated[4] for all the atoms from  $u=1$  to  $3N_{at}$  down to [8]. The perturbation matrices of the Hamiltonian of the first- and the second-order are prepared analytically. The

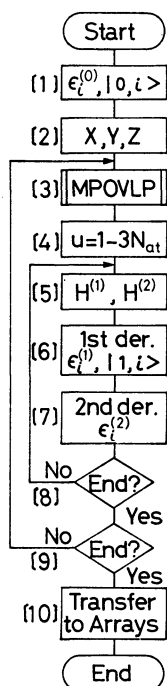


Fig. 3. Flow chart in a subroutine MPEHPT.

first-order perturbation eigenvalues and eigenvectors are calculated in [6] by following the algorithm of Carbo.<sup>7)</sup> The second-order perturbation eigenvalues are calculated from them and  $H^{(2)}$  by means of the above algorithm[7]. The derivatives of the total bond energy thus obtained are stored in arrays[10].

The algorithms in the subroutine MPZT are as follows. The vector,  $d$  in Fig. 1b that moves the representative point from P to B is given by the following equations (see Appendix):

$$d_i = -f_i'' \operatorname{sign}(f_i') \sum_i' \frac{|f_i'| |f_i''|}{\sum_i' (f_i'')^3} \quad \text{for } f_i'' \geq 0, \quad (10a)$$

$$d_i = 0 \quad \text{for } f_i'' < 0, \quad (10b)$$

where

$$f_i' = \frac{\partial E^{(0)}}{\partial q_i}, \quad (10c)$$

$$f_i'' = \frac{\partial^2 E^{(0)}}{\partial q_i^2}, \quad (10d)$$

and

$$d = (d_1, d_2, \dots, d_i, \dots, d_{3N_{at}}) \quad (10e)$$

In this processing, the summation regarding a few coordinates which give negative second derivatives is excluded. If the bottom thus found is outside the designated restriction in distance from P, the same procedure is iterated using renewed coordinates.

The direction of the steepest decent, and hence that of the path to the saddle point, is then easily determined by using  $f_i'$  values.

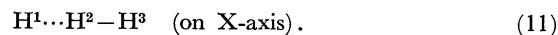
The subroutine ACTIVN judges the arrival at the saddle point, and then moves the system beyond that point. The arrival at the saddle point is recognized when none of the absolute values of the first derivatives exceed the optioned threshold value,  $EDRV1$ . In spite of the criteria of the saddle point given in Eqs. 1d and

1e, judgement by Eq. 1a alone is sufficient because the system is ascending and no minimum can appear before any saddle point, even if a basin exists. Then the system is moved for twice the distance restricted by constraint parameters along the vector from the initial point to the saddle point. Thus, the system goes to the opposite side of the PES, sufficiently far from the saddle point for the system not to return to the original side, but close enough to it not to fall down beyond the ridges on the PES in another valley, which would guide the system to an unexpected product.

The path down to the product is determined by either linear or quadratic approximation methods in the subroutine MPZT.

## Results and Discussion

The initial system is a linear molecule with interatomic distances of  $r_{12}=1.600 \text{ \AA}$  and  $r_{23}=0.740 \text{ \AA}$ , as



The total bond energy of the molecule was  $-4.6437 \text{ eV}$ , with the parameters for the resonance integral given above. The first and the second derivatives with respect to the  $x$ -coordinate are compared in Table 1 with those obtained by the method of finite differences with a shift of the  $x$ -coordinates,  $\delta$ , of  $\pm 0.025 \text{ \AA}$ . The agreement was proved excellent.

TABLE 1. COMPARISON OF DERIVATIVES WITH RESPECT TO  $x$  VALUES CALCULATED BY TWO METHODS

Method	Perturbation	Finite differences
First der. eV $\text{\AA}^{-1}$	1 <sup>a)</sup>	0.404
	2	0.113
	3	-0.517
Second der. eV $\text{\AA}^{-2}$	1	0.90
	2	37.0
	3	38.1

a) Atom ordinal. b)  $\delta = \pm 0.05 \text{ \AA}$ .

The parameters for processing were optioned as follows: the constraint parameters for atoms, which restrict their transfer distances in one step, were  $\pm 0.05 \text{ \AA}$ , and the threshold value,  $EDRV1$ , for the saddle point was  $0.1 \text{ eV/\AA}$ .

At first, the bottom of a valley was searched for with derivatives of the initial system; it was found at the geometry of  $r_{12}=1.592$  and  $r_{23}=0.759 \text{ \AA}$  with a total bond energy,  $TBE$ , of  $-4.6439 \text{ eV}$ , which is  $0.0002 \text{ eV}$  lower than the initial one. Although we used no control to inhibit the change in coordinates along either the Y- or the Z-axis, the bond angle (123) was actually  $180.0^\circ$ , and this angle remained unchanged throughout the reaction.

Secondly, a control variable was changed in order to search for the ascending path, and the system was transferred to new coordinates,  $r_{12}=1.540$  and  $r_{23}=0.759 \text{ \AA}$ , with  $TBE=-4.6223 \text{ eV}$ . The above interim results and succeeding iterations are shown on a contour map, Fig. 4, which had been separately prepared by a conventional grid method for demonstration. Up to

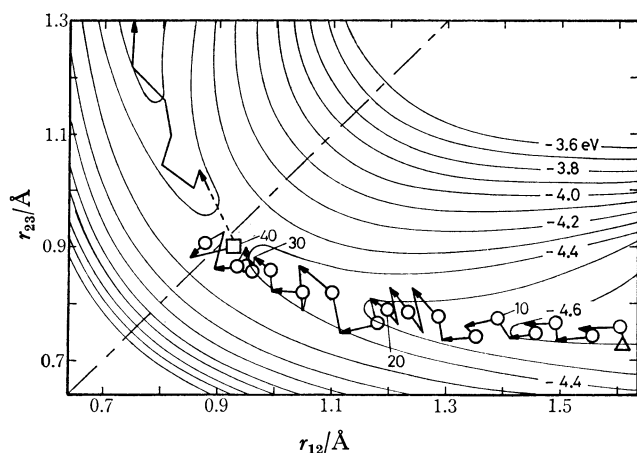


Fig. 4. Reaction path of  $H_3$  system beyond activated state.

$\triangle$ : Initial system,  $\circ$ : bottom of a valley.

$\leftarrow$ : Ascent during activation or decent during stabilization.

Numerals along the path indicate the iteration numbers, and those along the contour the  $TBE/eV$ .

TABLE 2. ATTRIBUTES OF ACTIVATED STATE SEARCHED FOR BY MATHEMATICAL PROGRAMMING

a. Activated state with restricted distance =  $0.05 \text{ \AA}$  and  $EDRV1 = 0.1 \text{ eV \AA}^{-1}$ .

- 1) Geometry:  $r_{12} = 0.9225$ ,  $r_{23} = 0.900 \text{ \AA}$ , and angle(123) =  $180.00^\circ$ .
- 2)  $TBE$ :  $-4.3771 \text{ eV}$ .
- 3) Derivatives along the X-axis:

Atom ordinal	1	2	3
First der./ $\text{eV \AA}^{-1}$	0.0459	-0.0207	-0.0252
Second der./ $\text{eV \AA}^{-2}$	7.75	-1.78	9.84

b. Symmetrical geometry.

- 1) Geometry:  $r_{12} = r_{23} = 0.91 \text{ \AA}$  and angle(123) =  $180.00^\circ$ .
- 2)  $TBE$ :  $-4.3768 \text{ eV}$ .
- 3) Derivatives along the X-axis:

Atom ordinal	1	2	3
First der./ $\text{eV \AA}^{-1}$	0.0530	0.0000	0.0530
Second der./ $\text{eV \AA}^{-2}$	8.88	-1.60	8.88

thirty iterations, the system, or the representative point, ascended nearly along the bottom of the valley leading to the saddle point. Meanwhile, two attempts to search for the bottom were carried out at the three iteration number of 16, 19, and 26. Beyond the iteration number of 30, the point began to wander on a fairly flat PES near the saddle point, designated by a square. At the iteration number of 40, all of the absolute values of the first derivatives became less than  $EDRV1$ , or  $0.1 \text{ eV/\AA}$  in this case, and the system was judged to be at the saddle point. The system had the geometry,  $TBE$ , and derivatives shown in Table 2a. The first derivatives well satisfy one of the criteria, Eq. 1a, the second derivatives satisfy Eqs. 1d and 1e, and the  $H^2$  atom is found to be related to the rupturing or forming bonds. The  $TBE$  of the reactant, that is,

a hydrogen molecule with an equilibrium interatomic distance and a hydrogen atom which is sufficiently far from the former, is found to be  $-4.759 \text{ eV}$  by the present MO; thus, the classical activation energy,  $E_A(\text{classical})$ , is  $0.382 \text{ eV} = 8.8 \text{ kcal/mol}$ , in good agreement with the experimental values.

No shallow basin seems to exist around the saddle point, judging from the wandering paths. Therefore, the true activated state is estimated to have a symmetric geometry of  $r_{12} = r_{23} = 0.91 \text{ \AA}$ . The attributes of the symmetric system are shown in Table 2b, where the first derivative of  $H^2$  is naturally zero and where the second derivatives for  $H^1$  and  $H^3$  were identical, the value being negative for  $H^2$ . The  $TBE$  is  $-4.3768 \text{ eV}$ , only  $0.0003 \text{ eV}$  ( $7 \text{ cal/mol}$ ) higher than that in Table 2a. Hence, this symmetrical system can be regarded as the true activated state.

The coordinates of the system were changed by  $0.1 \text{ \AA}$  by means of the algorithm mentioned above along the arrow with a broken line. Then the system began to go down along the bottom of a new valley to the product, as the control variable changed the algorithm to stabilization.

The total CPU time on a HITAC 8800/8700 for 40 iterations up to the saddle point amounted to 10 s.

This simplest example may be judged to verify the validity and usefulness of the new method for searching for the reaction path beyond the saddle point. The path shown in Fig. 4 is not a trajectory of the reaction, but only records the intermediate walks following the algorithm, because this method employs a static model instead of a dynamic treatment. The smoothed locus of open circles in Fig. 4, however, may give a fairly good reaction trajectory.

The author's thanks are due to Dr. Makoto Misono for his valuable discussion.

## Appendix

*Algorithm for Estimation of a Bottom of a Valley.* The energy  $E(\mathbf{d})$  at B in Fig. 1b, which was moved from P by a vector,  $\mathbf{d}$ , is expressed by the Taylor expansion by neglecting cross terms:

$$E(\mathbf{d}) \approx E(\mathbf{0}) + \sum_i^{3N_{\text{at}}} \left( f'_i d_i + \frac{1}{2} f''_i d_i^2 \right), \quad (\text{A1})$$

where  $E(\mathbf{0})$  denotes the energy at P.

The  $\mathbf{d}$  vector should be parallel to the  $\mathbf{f}''$  vector, where its elements are  $f''_i$ , negative values being replaced with zero. The sign of  $d_i$  should be decided so as to decrease the energy from P to B; hence, the  $d_i$  component is given by Eq. A2, taking into account the fact that the effective  $f''_i$  is non-negative:

$$d_i = \frac{k f''_i \text{sign}(-f'_i)}{\{\sum'_i (f''_i)^2\}^{1/2}}, \quad (\text{A2})$$

where  $\Sigma'$  denotes that the negative  $f''_i$  is excluded from summation and where  $k$  is an undetermined multiplier.

Equation A1 is converted to Eq. A3 by means of Eq. A2:

$$E(\mathbf{d}) = E(\mathbf{0}) + C \sum'_i \{ f'_i f''_i \text{sign}(-f'_i) k + \frac{1}{2} C (f''_i)^2 k^2 \}, \quad (\text{A3})$$

where  $C = \{\sum_i (f_i'')^2\}^{-1/2}$ .

The energy at B should be at its minimum along the PQ curves; hence,

$$\frac{dE(\mathbf{d})}{dk} = C \sum_i \{f_i' f_i'' \text{sign}(-f_i') + C(f_i'')^3 k\} = 0. \quad (\text{A4})$$

Thus,

$$k = - \frac{\sum_i f_i' f_i'' \text{sign}(-f_i')}{C \sum_i (f_i'')^3}. \quad (\text{A5})$$

Finally, the elements of  $\mathbf{d}$ —that is, the shifts in the coordinates—are derived as Eq. 10a from Eqs. A2 and A5, considering that  $f_i' \text{sign}(-f_i') = -|f_i'|$  and  $\text{sign}(-f_i') = -\text{sign}(f_i')$ .

## References

- 1) E.g., I. Shavitt, R. M. Stevens, F. L. Minn, and M. Karplus, *J. Chem. Phys.*, **48**, 2700 (1968); B. Liu, *ibid.*, **58**, 1925 (1973).
- 2) E.g., S. Glasstone, K. J. Laidler, and H. Eyring, "The Theory of Rate Processes," McGraw-Hill, New York (1941); S. Sato, *Bull. Chem. Soc. Jpn.*, **28**, 450 (1955); I. Yasumori, *ibid.*, **32**, 1103, 1110 (1959); R. N. Porter and M. Karplus, *J. Chem. Phys.*, **40**, 1105 (1964).
- 3) R. Hoffmann, R. Gleiter, and F. B. Mallory, *J. Am. Chem. Soc.*, **92**, 1460 (1970); H. Fujimoto, S. Yamabe, and K. Fukui, *Bull. Chem. Soc. Jpn.*, **45**, 1566 (1972).
- 4) K. Fukui, *J. Phys. Chem.*, **74**, 4161 (1970); "The World of Quantum Chemistry," ed by R. Daudel and B. Pullman, D. Reidel Publ. Co., Dordrecht, Holland (1974), p. 113.
- 5) R. Hoffmann, *J. Chem. Phys.*, **39**, 1397 (1963).
- 6) M. Salomon, *J. Chem. Phys.*, **51**, 2406 (1969).
- 7) R. Carbo, *Theor. Chim. Acta (Berl.)*, **17**, 74 (1970).